



Long-Term Low-Cycle Corrosion Fatigue of Steel 08Kh18N10T and its Welded Joints in Water of High Parameters

Vladimir M. Filatov¹⁾, Aleksandr V. Zelensky²⁾

¹⁾ ENES, Moscow, Russia

²⁾ VTI, Moscow, Russia

ABSTRACT

Steel 08Kh18N10T (similar to steel 321SS) and the weld metal of full-scale pipe of the WWER-440 main circulation pipeline were tested for fatigue in air environment (300 °C) and in deoxygenated water (9 MPa, 300 °C). Cantilevered specimens were loaded in a displacements-controlled symmetrical triangular cycle. The strain rate during tests in water was $1.1 \cdot 10^{-3} - 6.7 \cdot 10^{-2} \% s^{-1}$. Given equal strain amplitudes, the number of cycles to failure in water, as compared with air testing, is reduced by a factor of 8-13 at the most with strain rate decrease. The results of testing steels 18-8 in PWR water show fair agreement with fatigue curves according to the equation based on the ANL model. This paper presents equations for calculating curves in case of loading in water and air, as well as design fatigue curves for austenitic stainless steels 18-8 under the given conditions. Fatigue crack growth was studied as found in the base metal and the weld in air, with the asymmetry coefficient $R = 0.1$ and 300 °C. The results were compared with the design curves for conditions of air and PWR water environment as well as with the design curve in air, calculated by the ASME Code.

KEY WORDS: corrosion fatigue, strain rate, temperature, oxygen concentration, crack growth.

INTRODUCTION

Standards and codes for strength analyses of nuclear plant components include design fatigue curves for loading in air, whereas components of plants with light-water reactors (LWR), commonly made of austenitic stainless steels 18-8 (SS), are cyclic loaded in water environment.

Cycling loading in water of high parameters at a high strain rate and with holdups at maximum strain was found to have no effect on the number of cycles to failure of steel 08Kh18N10T and weld metal [1]. Analysis [2] has shown that strain rate decrease leads to a considerable reduction in the number of cycles in water of high parameters.

The fatigue curves according to Langer equation with the use of reduction in area and rupture strain of the oxide film under low-rate tension in water of high parameters were reasonably consistent with the results of low-cycle tests of steel 17 MnMoV64 in water [3].

TEST MATERIALS AND SPECIMENS

Specimens were cut out from a tube (with the outer diameter of 560 mm and wall thickness of 34 mm) in axial direction and from a circumferential weld (electrode EA-400/10U). The yield strength $R_{p0.2}^T$, ultimate strength R_m^T , elongation A^T and reduction in area Z^T were determined on specimens with the working length of 15 mm and diameter of 3 mm; the cyclic bending specimens (58x5x2 mm) had a one-sided groove 31.5 mm in radius and 0.25 mm in depth in the bend plane. The fusion line on the weld fusion zone specimens ran in the middle of the groove.

Table 1. Mechanical characteristics at 300 °C

Material	$R_{p0.2}^T$, MPa	R_m^T , MPa	A^T , %	Z^T , %
Steel 08Kh18N10T	312	405	32.0	64.0
Weld metal	303	437	26.5	56.0
Fusion zone metal (08Kh18N10T)	310	435	25.0	68.5

Compact specimens 30 mm thick produced for crack growth studies had an edge notch (in the axial direction of the tube) 15 mm in depth from the load application line and 3 mm in width with a straight front and a radius of 0.25 mm at the tip.

TESTING FACILITIES AND PROCEDURE

Air tests were staged on the Schenck-Hydropuls system machine at 300 °C and a frequency of 10 Hz.

Eight cantilevered specimens were tested simultaneously in a displacements-controlled symmetrical cycle with automatic failure recording. Displacement was determined by a calibration curve derived from strain gauge measurements at room temperature on steel 08Kh18N10T, weld metal and fusion zone specimens.

Growing of 3 mm cracks in compact specimens was arranged in 0.5 mm steps, with the load reduction at each step; the range of the stress intensity factor at the final step was $\Delta K = 19 \text{ MPa } \sqrt{\text{m}}$.

Fatigue tests of specimens exposed to water of high parameters were conducted in an autoclave made of steel 08Kh18N10T, placed in a circuit with natural circulation, which included a vessel with electric heaters, a cooler, a pump for initial pressure generation and circuit makeup, a pressuriser, a safety valve, and a water sampler. Twelve cantilevered specimens were tested simultaneously at equal displacements and with automatic failure recording. The time of triangular symmetrical cycle of displacements was equal to 0.5, 3 and 30 minutes.

The temperature and pressure in the circuit were 300°C and 9 MPa, respectively. The circuit was filled with purified water (pH = 6...7, chloride concentration ~ 0.05-0.1 ppm, total hardness ≤ 10 ppm). Following deaeration, the temperature and pressure were raised to specified values (over 7-10 h), whereupon the circuit was kept at the set parameters for 18-20 h till the beginning of the tests. With such a procedure, the initial oxygen concentration was reduced considerably. Ref. [4] indicates that it takes 40 h to have water in an autoclave (08Kh18N10T) completely deoxygenated at 340°C and 3.5 MPa without deaeration [4]. Analysis of water samples from the circuit confirmed low oxygen concentration (<0.05 ppm).

TEST RESULTS

Decrease of cyclic strength in water of high parameters was determined by coefficient $F_{en} = N_a/N_w$, where N_a , N_w numbers of cycles to failure in air and water with equal strain amplitude e_a , respectively ($F_{en} \geq 1$).

Figure 1 presents the values of F_{en} for 08Kh18N10T, weld metal and fusion zone. Coefficient F_{en} becomes smaller with strain rate increase, $\dot{\epsilon} \approx 4e_a/t_c$, where t_c is the cycle duration. A somewhat greater F_{en} decrease with amplitudes of 0.7 and 1.2 % is accounted for by the shorter testing time (50...25 h), which was not long enough for oxygen concentration to reach its minimum.

According to the Regulations [5], the effect of working environment must be allowed for in check up calculations, including fatigue analysis, based on experimental data. With the test results (Fig. 1) made available in 1991, the effect of water environment on fatigue of components made of steel 08Kh18N10T came to be allowed for by reducing to one-tenth the number of cycles permitted by the Regulations [5] without regard for the ambient conditions.

EQUATIONS FOR FATIGUE CURVES AND CRACK GROWTH

The results of fatigue testing of steels 18-8 under strain-controlled uniaxial tension-compression in reactor water, published in 1995-2000 [6-8], point to a set of parameters with definite effects on the cyclic strength of the steels in question, which include oxygen concentration in water (OC), strain rate in the tension half-cycle ($\dot{\epsilon}$), and water temperature (T).

Using a statistical model based on Langer equation [9], the equation of the mean fatigue curve for steels 304SS and 316SS with regard to water effects ($T \leq 350^\circ\text{C}$) will be written as:

$$e_a = 24,47 \exp(0,0677\dot{\epsilon}^*) N^{-0,505} + (e_a)_{th} \quad (1)$$

where $\dot{\epsilon}^* = 0$ at $\dot{\epsilon} > 1\% \text{ s}^{-1}$; $(e_a)_{th} = 0.12\%$ with symmetrical cycle;
 $\dot{\epsilon}^* = \ln(\dot{\epsilon})$ at $10^{-3} \leq \dot{\epsilon} \leq 1\% \text{ s}^{-1}$; $(e_a)_{th} = 0.103\%$ with regard to mean stress according to
 $\dot{\epsilon}^* = \ln(10^{-3})$ at $\dot{\epsilon} < 10^{-3}\% \text{ s}^{-1}$; modified Goodman's diagram

For loading in air environment: $(e_a) = 29,33 N^{-0,505} + e_{ath} \quad (2)$

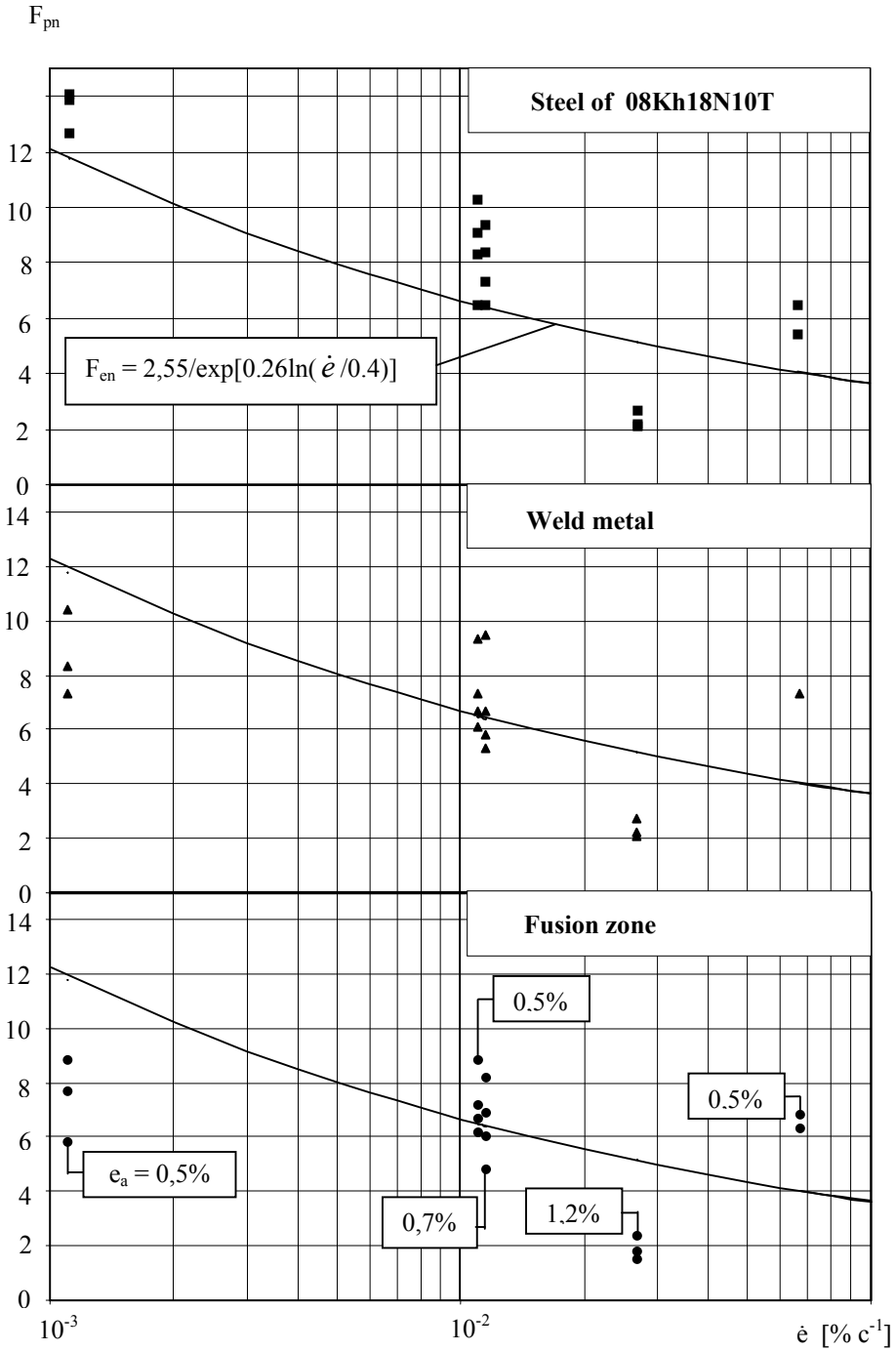


Fig. 1. F_{en} factors for some zones of 08Kh18N10T steel welded joints

Another paper [8] offers an equation of the mean fatigue curve for the same steels in water of high parameters:

$$e_a = 17,14 \exp(0,493 \cdot T^* \cdot \dot{\epsilon}^* \cdot 0^*) N^{-0,493} + (e_a)_{th} \quad (3)$$

where	$T^*=0$	at $T < 180^\circ\text{C}$;	$\dot{\epsilon}^* = 0$	with $\dot{\epsilon} > 0,4\% \text{ s}^{-1}$;
	$T^*=(T-180)/40$	at $180 \leq T < 220^\circ\text{C}$;	$\dot{\epsilon}^* = \ln(\dot{\epsilon}/0,4)$	with $4 \cdot 10^{-3} \leq \dot{\epsilon} \leq 0,4\% \text{ s}^{-1}$;
	$T^*=1$	at $220 \leq T \leq 350^\circ\text{C}$;	$\dot{\epsilon}^* = \ln(10^{-3})$	with $\dot{\epsilon} < 4 \cdot 10^{-3}\% \text{ s}^{-1}$;
	$0^*=0$	at $\text{OC} \geq 0.05 \text{ ppm}$;	$(e_a)_{th} = 0.126\%$	with symmetrical cycle;
	$0^*=0.26$	at $\text{OC} < 0.05 \text{ ppm}$;	$(e_a)_{th} = 0.1\%$	including the effect of mean stress

while in air environment:
$$e_a = 18,44 N^{-0,493} + (e_a)_{th} \quad (4)$$

Coefficient F_{en} from relations (1), (2) [9] is equal to:

$$F_{en} = 1,432 / \exp(0,134 \dot{\epsilon}^*) \quad (5)$$

and from (3), (4) [8]

$$F_{en} = 2,55 / \exp(T^* \cdot \dot{\epsilon}^* \cdot 0^*) \quad (6)$$

Figure 1 displays relation (6) at $T = 300^\circ\text{C}$ and $\text{OC} < 0.05 \text{ ppm}$. Coefficient F_{en} (5) takes on a smaller value. The test results are in fairly good agreement with relation (6) for steel 08Kh18N10T and in somewhat worse agreement for the weld metal and fusion zone.

The fatigue curve equation for crack initiation in air environment, of the Manson type, appears as:

$$e_a = e_c^T (4N)^{-m} + (E^T)^{-1} (R_c^T - \sigma_{F_{max}} \cdot i_\sigma) [(4N)^{m_e} - i_\sigma]^{-1} \quad (7)$$

where	$e_c^T = 0.5 \ln 100 / (100 - Z_c^T)$;	E^T – elastic modulus;
	$Z_c = Z^T$ with $Z \leq 30\%$, $Z_c^T = 15 + 0.5Z^T$ with $Z > 30\%$;	$R_c^T = R_m^T (1 + 0.014Z_c^T)$;
	$m = 0.5$ with $R_m^T < 700 \text{ MPa}$;	$m_e = 0.132 \lg(2.5 + 0.035Z_c^T)$;
	$\sigma_{F_{max}}$ – maximum stress of the cycle;	
	$i_\sigma = 0$ with $E^T \cdot e_a \geq \sigma_{F_{max}}$ or $E^T \cdot e_a \geq R_p^T$;	$i_\sigma = 1$ with $E^T \cdot e_a < \sigma_{F_{max}} \leq R_p^T$.

It is acceptable to set $e_c^T = 0,005 Z^T$.

With a specified amplitude e_a , the number of cycles $N = \min(N_1 \text{ for } i_\sigma = 0; N_2 \text{ for } i_\sigma = 1)$.

The fatigue curves from equation (7) are consistent with the experimental curves for steels of various classes exposed to air [10]. The value of R_p^T defines the boundaries of cyclic elastic loading. The loading history of a component may include elastic and elastic-plastic loading cycles, with the latter leading to hardening or softening. Material behaviour depends on a number of factors, such as initial condition, temperature, and strain rate. The elastic loading boundaries are approximately defined by the value of $R_p^T = 0.5(R_{p02}^T + R_m^T)$. The minimum temperature of the cycle is taken in the case of non-isothermal loading.

Equations (1) – (4) were obtained by processing of data from a test with a strain-controlled steady-state cycle; no tests were conducted for an asymmetric cycle. Given $N \leq 10^6$, it was found for the tested steels that $E^T \cdot (e_a)_{th} \geq R_{p02}^T$, which is why analysis within this range will be confined to the symmetric strain cycle.

With regard to the effect of water environment, the fatigue curve equation appears as:

$$e_a = e_c^{20} (4F_{en} \cdot N)^{-m} + (E^T)^{-1} \cdot R_{cF}^T (4N)^{-m_{eF}} \quad (8)$$

where F_{en} is determined by relation (6), $R_{cF}^T = R_m^T (1 + 0.014Z_F^T)$, $m_{eF} = 0.132 \lg(2.5 + 0.035Z_F^T)$.

The value of Z_F^T is found from relations:

$$Z_F^T = Z_c^T \text{ with } Z_c^T \leq 30\%, \quad Z_F^T = 2(Z_c^T - 15) \text{ with } Z_c^T > 30\%, \quad Z_F^T \leq Z^T$$

where $Z_c^T = 100[1 - \exp(-2e_c^{20} \cdot F_{en}^{-m})]$.

It is acceptable to set $Z_F^T = Z^{20} \cdot F_{en}^{-m}$.

For carbon steels (CS) and low-alloy steels (LAS) $E^T \cdot (e_a)_{th} \approx 1,2 R_{-1}^T$ [8], where R_{-1}^T is the fatigue limit. For SS $(e_a)_{th} \approx 0.16 - 0.18\%$ [7, 8], which is higher than $(e_a)_{th}$ in equations (1) - (4).

The value of $(e_a)_{th} = 0.18\%$ was determined in an indirect way [7]; durability was found to be unaffected by the In equation (8), elastic strain depends on N , and with $N=10^7$, it is taken that $E^T \cdot (e_a)_{th} = R'_{-1} = 0.4R'_m$.

The process of component loading consists of successive half-cycles with various e_a , separated by steady state parts with possible superposition of vibrations, when the damaged oxide film may be cured. The environmental effects show up during oxide film failure ($e_a > (e_a)_{th}$) and opening of a mechanically small crack to let the medium in.

The fatigue curve allowing for the effect of water environment will be defined by equations (7), (8). With specified e_a , the value of N will be equal to the least of the two values found from these equations.

The fatigue curves from equations (1), (3), (8) in PWR water environment (300 °C, OC < 0.005 ppm) with $\dot{\epsilon} \leq 4 \cdot 10^{-4} \% s^{-1}$ in the tension half-cycle and the fatigue curve from equation (7) in air with $i_\sigma = 0$ are compared in Fig. 2 with the results of testing steels 304SS [11] and SUS 304 [6] in a symmetric strain cycle (288, 325° respectively) in water and in air. In the region of $e_a = 0.15 \dots 0.25\%$, there are no results for $\dot{\epsilon} = 4 \cdot 10^{-4} \dots 1 \cdot 10^{-3} \% s^{-1}$.

The curves were calculated using the characteristic of steel SUS304 [6]:
 $R'_{p02} = 161$ MPa, $R'_{m} = 447$ MPa, $Z^{325} = 64.7\%$, $Z^{288} = 70.4\%$, $E^{325} = 1.77 \cdot 10^5$ MPa.

The crack initiation curve (Eq. 7) forms an underside envelope for the air testing data corresponding to the so-called “engineering-size” crack in specimens. This is a through-wall crack in tubular specimens with the wall thickness of 3 mm [6, 11], and a crack 3 mm deep in solid specimens [8].

The curves of equations (2), (8) are consistent with the results of tests in water of high parameters with the strain rate adopted in the calculations, which is not the case with curve 1 of equation (1).

The tests [6, 8, 11] were staged at constant T , e_a , $\dot{\epsilon}$, OC, wherefore tests are to be conducted to determine the effect of unsteady-state loading on the value of $(e_a)_{th}$ with summation of the corrosion fatigue damage. Tests with $e_a < (e_a)_{th}$ are required to confirm the hypothesis on the crucial role of the metal’s fatigue resistance. Applicability of Goodman’s diagram to calculation of loading in water environment has found no experimental support.

Equations (6) – (8) are used for assessing the effect of water environment on the fatigue characteristics of Russian steels 18-8 similar in composition to steels 304SS and 316SS.

The design fatigue curves according to the Regulations [5] are derived using specified values of R'_{p02} , R'_m , Z^T (which are normally smaller than in real life), data of relevant standards or those contained in the obligatory Annex to the Regulations. Hence, they set $Z'_c = Z^T$, if $Z^T \leq 50\%$, or $Z'_c = 50\%$ with $Z^T > 50\%$. Coefficients $n_\sigma = 2$ or $n_N = 10$ (whichever is more conservative) are included in determining the permissible strain amplitude $[\sigma_{aF}] = E^T \cdot e_a$, quasi-elastic in the elastic-plastic area, or the number of cycles $[N]$ to compensate for data variations and difference between the laboratory specimen and real component in surface condition and dimensions.

The design curves for SS derived from equations (6) - (8) with regard to the maximum effect of mean stress at $\dot{\epsilon} = 4 \cdot 10^{-4} \% s^{-1}$, are given in Fig. 3.

With $[\sigma_{aF}] < 100$ MPa, the values of $[N]$ are determined by the metal’s cyclic strength and are not affected by the water environment. The same equations with the corresponding coefficient F_{en} are in use for carbon steels and low-alloy steels [8].

Tests of compact specimens demonstrated the rate of crack growth in steel 08Kh18N10T to be higher than in the weld metal and fusion zone (Fig. 4).

The test results support the validity of the adopted design curves for fatigue crack growth. The design curve for steel 08Kh18N10T and its welds is only slightly different from the curve of the ASME Code. The effect of deoxygenated water is allowed for by increasing the rate 2 times [13]. According to Ref. [14], the rate is 2-3 times higher at the most in deionised water than in air environment with $\Delta K = 20-30$ MPa \sqrt{m} . Outside this interval the difference is smaller.

CONCLUSION

Fatigue curve equations for design of nuclear plant components were derived with the use of experimental data showing the effect of LWR water coolant on the fatigue characteristics of steels 18-8. The fatigue curves calculated by these equations are consistent with the results of tests. Design curves for conditions of loading in air and LWR water environment are presented in this paper.

The relation involved in calculation of fatigue crack growth in steels 18-8 is experimentally supported and agrees with the relevant relation in the ASME Code.

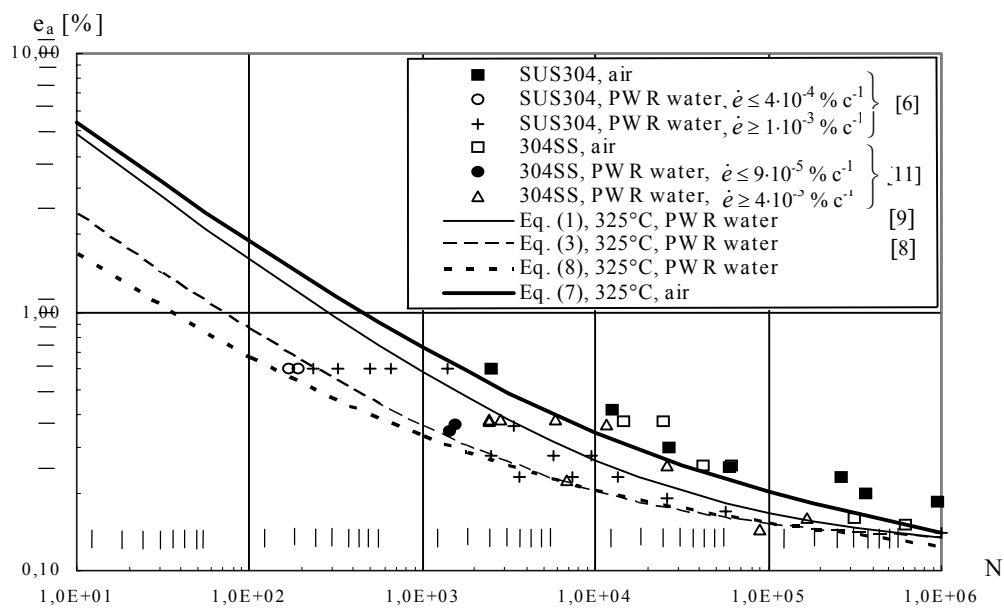


Fig. 2. Comparison of experimental results and calculated SSs fatigue curves (the strain-controlled symmetrical cycle)

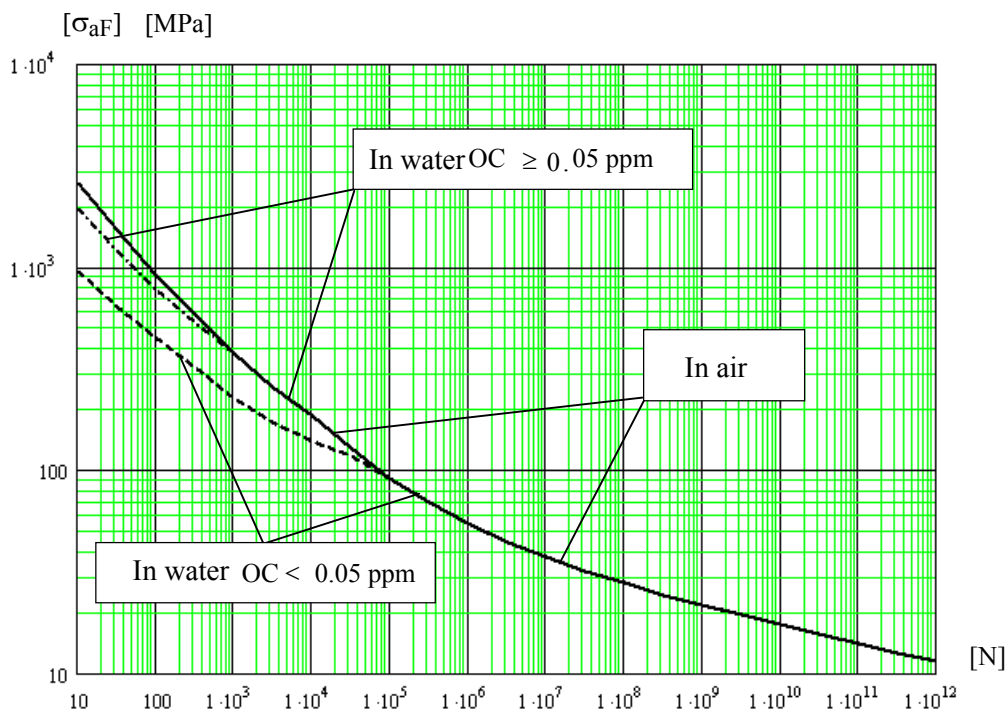


Fig. 3. Design fatigue curves for austenitic stainless steels

at $R_m^T \geq 350 \text{ MPa}$; $R_{p0.2}^{20} \leq 200 \text{ MPa}$; $R_{p0.2}^{20}/R_m^T \geq 0.4$; $Z^{20} \geq 45\%$; $Z^T \geq 40\%$, $E^T \geq 175 \text{ GPa}$; $T \leq 350 \text{ }^\circ\text{C}$

REFERENCES

1. Filatov V.M., Zelensky A.B., Low Cycle Fatigue of Structural Materials in Water Operating Environments, Proc. of the Third International Atomic Energy Agency Specialists Meeting on Subcritical Crack Growth, NUREG/CP – 0112, A NL-90/22, v. 1, pp 215 – 222, Moscow, Russia, May 14-17, 1990.
2. Filatov V.M., Gorynina L.V., Fatigue failure of structural materials in light-water reactor environment (Review), M., NIIFORMENERGOMASH, 1983, No. 86.
3. Filatov V.M., Calculation and Experimental Evaluation of Long-Term Corrosion Cycle Strength , Zavodskaya Laboratoriya, № 9, 1991, pp 66-68.
4. Gerasimov V.V. et al. Corrosion cracking of steel 1Kh18N10N. In: “Corrosion of reactor materials”, Gosatomizdat, M., 1960.
5. Rules and Regulations in Nuclear Power Engineering. Regulations for Strength Analysis in Nuclear Power Plant Equipment and Piping. PNAE G-7-002-86, Energoatomizdat, M., 1989.
6. Kanasaki H. et al., Fatigue Lives of Stainless Steels in PWR Primary Water, Trans. of the 14th Intern.Conf. on Struct. Mechan.in Reactor Technol. (SMiRT14), v. DO7/1, pp. 473-483, Lyon, France, Aug.1997.
7. Kanasaki H. et al., Effects of Strain Rate and Temperature Change on the Fatigue Lives of Stainless Steels in PWR Primary Water, *ibid.*6.
8. Chopra O.K., Muscara J., Effects of Light Water Reactor Coolant Environments on Fatigue Crack Initiation in Piping and Pressure Vessel Steels, Proc. of ICONE 8, 8th Intern. Conf. on Nucl. Engin., ICONE-8300, Baltimore, MD USA, April 2-6, 2000.
9. Keisler J.M., Chopra O.K., Shack W.J., Statistical Models for Estimating Fatigue Strain – Life Behavior of Pressure Boundary Materials in Light Water Reactor Environments, Nuclear Engineering and Design , 167(1996), pp. 129-154.
10. Filatov V.M., Allowable Stresses and Design Fatigue Curves in Russian Regulations for Strength Analysis and ASME Code for Nuclear Power Plant Components – 4th Intern.Conf. on Material Science Problems in NPP Equipment. Production and Operation., St.-Petersburg, Russia, June 16-23 1996.
11. Chopra O.K., et al., Current Research on Environmentally Assisted Cracking in Light Water Reactor Environments, Nuclear Engineering and Design, 194 (1999), pp.205-223.
12. ASME Boiler and Pressure Vessel Code, Sec.XI, Rules for Inservice Inspection of Nuclear Power Plant Components, ASME, NY, 1995.
13. Section XI Task Group for Piping Flaw Evaluation, ASME Code, Evaluation of Flaws in Austenitic Steel Piping, J.Pres.Ves. Technol, v.108, 1986, pp. 352-366.
14. Grin Ye.A., Dmytrakh I.N., Crack development behavior in steel pipelines of power plants with cyclic loading and coolant impacts. *Electrichestkiye stantsii*, No. 6, 1991, p.73-76.